

Thermoplastic - PDMS polymer covalent bonding for microfluidic applications

Borut Pečar, Matej Možek and Danilo Vrtačnik

University of Ljubljana, Faculty of Electrical Engineering, Laboratory of Microsensor Structures and Electronics, Ljubljana, Slovenia

Abstract: Two room-temperature bonding processes for thermoplastic - PDMS polymer covalent bonding based on the organic substrate surface functionalization by means of organofunctional silanes APTES and amine-PDMS linker were developed and applied. The efficiency of covalent bonding was evaluated by measuring water contact angles on oxygen plasma pretreated surfaces and by measuring burst pressure on fabricated test devices. Developed amine-PDMS linker bonding process resulted in bond strength of 5 bar and 2 bar on continuous pressure of air and water respectively, while water initiated the hydrolysis of covalent bonds established via the modified APTES bonding process. Both bonding processes were applied on piezoelectric micropumps where glass substrate was replaced by thermoplastic substrate. Micropumps employing amine-PDMS linker exhibit no deterioration in their performance after eight weeks of continuous operation.

Keywords: PDMS; WCA; APTES; thermoplastics; covalent bonding; micropump

Kovalentno spajanje termoplasta s PDMS polimerom za mikrofluidne aplikacije

Izvleček: Raziskali, razvili in vpeljali smo dva nizko temperaturna postopka kovalentnega spajanja termoplasta in PDMS polimera, ki temeljita na funkcionalizaciji organske površine preko organofunkcionalnega silana APTESa in amino-PDMS povezovalca. Učinkovitost površinske aktivacije, ki je ključna za učinkovit kovalenten spoj, smo ovrednotili z merjenjem omakalnih kotov vodnih kapelj na površini vzorcev pred in po aktivaciji površin v kisikovi plazmi. Za ovrednotenje kvalitete spoja smo na namensko izdelanih testnih čipih izvedli tlačne in porušitvene teste. Amino-PDMS povezovalac je zagotovil obstojnost spoja ob stiku z vodo, medtem ko so vezi vzpostavljene preko APTESa kljub dodatni toplotni obdelavi po nanosu in modifikaciji parametrov plazemske aktivacije površin razpadle. Razvita postopka spajanja smo vpeljali v proces izdelave piezoelektričnih mikročrpalk. Piezoelektrične mikročrpalke izdelane s postopkom amine-PDMS povezovalca po osmih tednih neprekinjenega delovanja ne izkazujejo upada pretočne zmogljivosti.

Ključne besede: PDMS; WCA; APTES; termoplast; kovalentno spajanje; mikročrpalka

* Corresponding Author's e-mail: borut.pecar@fe.uni-lj.si

1 Introduction

Plastics are indispensable in mass production of microfluidic devices due to their robustness, light weight, optical transparency, simplicity of molding and cost efficiency [1]. Plastics rigidity enables a variety of reliable external interface options, such as manifold integration, direct barbed tubing connections, and gasket connectors [2]. In addition, thermoplastic (TP)-polydimethylsiloxane (PDMS) assemblies have a number of advantages over homogeneous assemblies. The combined surface properties of the two materials, for example, could provide an optimal environment for con-

ducting cell-based research necessitating precise fluid control for targeted cell or biomolecule immobilization [3].

Many strategies for plastic-PDMS bonding have been previously reported, such as sol-gel coating approach, chemical gluing approach and organofunctional silanes approach [4, 5]. First approach requires multiple coating procedures as well as complex technology. Second approach creates chemically robust amine-epoxy bonds at the interface at room temperature, however, two silane-coupling reagents are required and both

surfaces had to be oxidized prior to chemical modification. Third approach requires only one coupling agent. In this approach, the most widely used organofunctional silane is 3-amino propyltriethoxysilane (APTES), aminosilane frequently employed in covalent bonding of organic films to metal oxides [6].

However, TP-PDMS covalent bonds established via organofunctional silanes are prone to degradation over prolonged period in aqueous environment which might limit the use in specific microfluidic applications.

Few studies attempted to increase hydrolytic stability of APTES by mixing it with complex agents such as BTISPA, BTMSPA, BTESE [2] or GPTMS [7]. Hydrolytic resistance of APTES mixed with BTISPA improved to hydrolytically stable bonds over a range of 0 to 15 pH when BTISPA was prevailing in the mixture. Authors attributed increased hydrolytic resistance to the greater cross-link density for bis-silanes. APTES mixed with GPTMS yielded higher bond strength as compared to APTES, but did not improved hydrolytic stability [8].

Being aware of reported limited hydrolytic resistance of APTES [2, 7], we tried to introduce additional post-deposition heat treatment and modification of post-deposition plasma treatment that might overcome this disadvantage and provide the bond strength sufficient for specific application e. g. in the range of 0.5-0.7 bar. The advantages of employing APTES linking agent include easy availability of the product and well established bonding process due to substantial popularity in microfluidic community.

In this work, approach of employing two organofunctional silanes, APTES and poly [dimethyl siloxane-co-(3-aminopropyl) methyl siloxane (amine-PDMS linker) for bonding PDMS elastomer to TP substrates via methanol aligning medium was developed and applied. Amine-PDMS linker incorporates an amine functionality at one terminal and a segment of low molecular weight PDMS at the other, which might provide better hydrolytic bond stability [3]. Surface properties of TPs and PDMS were analyzed by measuring the water contact angles (WCA). The bond strength and bond hydrolytic stability were evaluated by delamination and burst pressure tests. Both bonding processes were further improved and applied on piezoelectric micropumps, where supporting bottom glass was replaced by TP substrate.

2 Experimental

2.1 Materials

In the presence of amine in organofunctional aminosilane bonding process, thermoplastics undergo

aminolysis followed by chain scission of the carbonyl backbone, forming a strong urethane bond. Therefore, not all thermoplastics, but only thermoplastics that can undergo aminolysis are suitable for the purpose. For TP substrates, optically transparent 2 mm thick Polycarbonate (PC), Acrylonitrile butadiene styrene (ABS) and Poly methyl methacrylate (PMMA) from INEOS Styrolution Group GmbH were employed.

In all experiments, a PDMS Sylgard® 184 two-part kit consisting of a pre-polymer (base) and a cross-linker (curing agent) from Dow Corning Corporation mixed at a ratio 10:1 was applied. For surface functionalization of plastic substrates, a commercial solution of APTES (Sigma Aldrich) and amine- PDMS linker (Sigma Aldrich) were used. In bonding processes, methanol and DI of technical purity were applied.

2.2 Surface wettability measurements

As argued by Garbassi et al. [9], the oxidation of the surface layer increases the concentration of hydroxyl groups which leads to the formation of strong intermolecular bonds. As the silanol groups are polar in nature, they make the exposed surface highly hydrophilic and this can be observed by measuring WCAs [10]. Those WCAs were found in direct correlation with bond strength [11].

For WCA determination a method was developed which included photographing of droplets on inves-

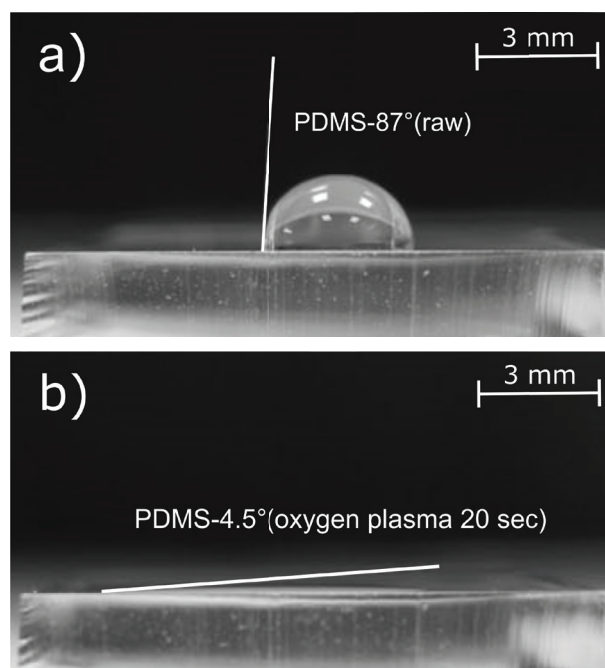


Figure 1: Micrograph (camera Nikon e990) of water droplet on raw PDMS surface (a) and on oxygen plasma treated PDMS surface (b).

tigated surfaces. The images of the droplet were analyzed by computer software “ImageJ” and “ContactAngle” plugin from points marked along the droplet-air interface to calculate the contact angle at the droplet-surface interface.

An example of WCA measurement on raw PDMS and on PDMS treated in oxygen plasma (20 sec, 0.8 mbar, 40W) is shown in Fig. 1. For all plasma treatments, ATTO Low Pressure Plasma Systems Diener electronic GmbH was employed.

2.3 Bonding process

In order to overcome reported limited hydrolytic resistance of APTES [2, 7], additional post-deposition heat treatment and modification of post-deposition plasma treatment were introduced in the bonding process. The process flow for TP-PDMS sandwich covalent bonding is schematically shown in Fig. 2. First, TP substrates were cleaned in ultrasonic bath, followed by silylation of the surfaces through the use of organofunctional silanes. In order to achieve good adhesion, TPs were pre-activated in oxygen plasma, resulting in the hydrophilization of the TP surfaces.

TP sheets were then immersed in the APTES (5% per volume) or coated with amine-PDMS linker and addi-

tionally heated to 60 °C for 20 min. Such an additional post-deposition heating step was expected to increase the number of established urethane bonds, especially between TP and APTES where bonds are prone to hydrolytic decay. Unlinked organofunctional silanes were washed away with isopropyl alcohol in ultrasonic bath. Both PDMS and functionalized TP substrate surfaces were again activated in the oxygen plasma. Post-deposition plasma treatment was prolonged to 1 min at increased pressure of 2 mbars and increased power of 50 W in order to increase the formation of Si–OH groups on both surfaces (Fig. 2 b). For all further oxygen plasma treatments, modified parameters were employed.

After plasma activation, the activated surfaces of the two substrates were brought into contact, using methanol as an aligning medium (Fig. 2 b). After methanol evaporation, covalent bonds were formed which were then additionally stabilized by curing at 80°C for 1 h in laboratory furnace.

2.4 Characterization of the bond strength

The bond strength was evaluated by performing delamination and burst pressure tests. Fig. 3 shows PDMS residues on ABS substrate after the PDMS elastomer was delaminated. In this particular case, APTES was employed as a linking agent. It was presumed that the area of PDMS residues left on the TP surface was directly related to bond strength. No obvious correlation between TP type and bond strength was found by delamination tests.

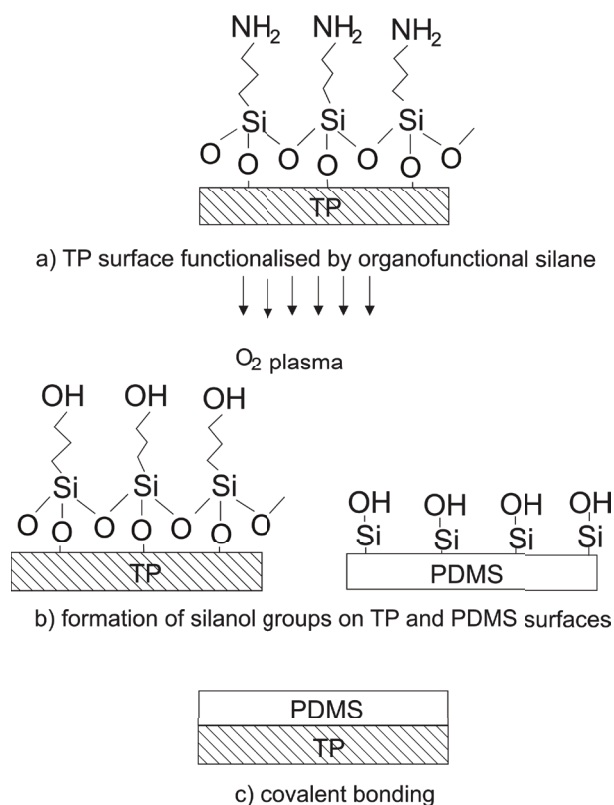


Figure 2: Process flow for TP-PDMS sandwich covalent bonding.

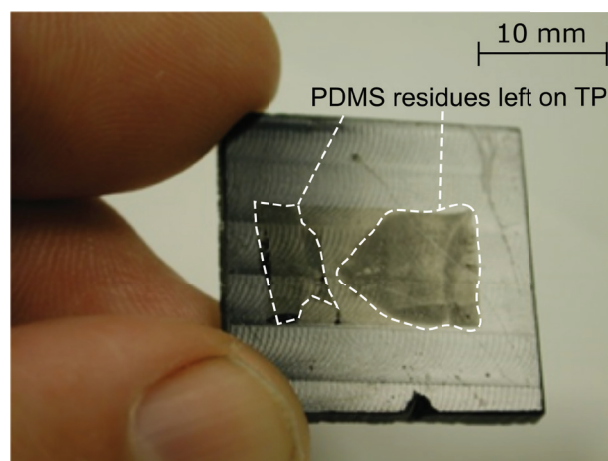


Figure 3: Photography of PDMS residues on ABS substrate after the PDMS elastomer was delaminated.

Next, the bond strengths were measured using burst pressure test devices. Top view and lateral cross-section of designed burst pressure test device is shown in Fig. 4.

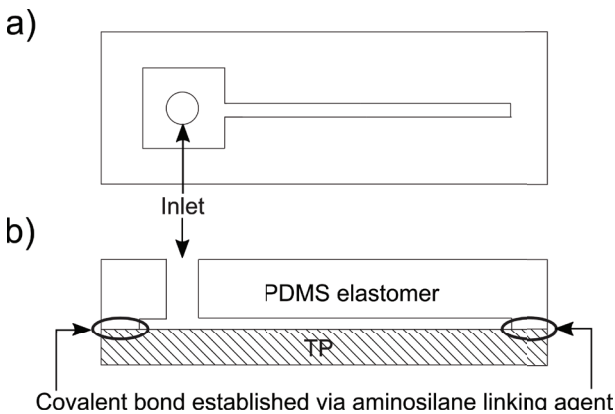


Figure 4: Schematics illustration of burst pressure test device. Top view (a) and lateral cross section (b).

Devices were fabricated by employing replica molding technique. Silicon mold for PDMS cast was fabricated by one-step photolithography and deep reactive ion etching (DRIE). Casted PDMS elastomer layers with microstructures (square-shaped inlet chambers with microchannels) were thermally cured at 60 °C for 1 hour and bonded to TP substrates applying bonding process described in Sect. 2.3.

Pressure regulated air supply was connected to the inlet of the test device and the pressure at which the device failed was determined. Device always failed at the region where the square-shaped inlet chamber narrows into the channel indicated by arrow position in Fig. 6. Here, the structural stress caused by applied fluidic pressure was the largest.

The region of failure was further confirmed by employing 3-D numerical simulations in COMSOL Multiphysics software. Test device behavior can be explained considering two different physics models coupled together. Fluid flow is described by the Navier-Stokes equation

$$\rho \frac{\partial \mathbf{v}}{\partial t} + \rho(\mathbf{v} \cdot \nabla)\mathbf{v} = \nabla \left[-p\mathbf{I} + \mu \left(\nabla \mathbf{v} + (\nabla \mathbf{v})^T \right) \right] + \mathbf{F} \quad (1)$$

where the left hand side represents contribution of the force acting on a differential volume of a fluid and the inertial force. \mathbf{v} is the fluid velocity, ρ density, p pressure and μ dynamic viscosity. Equation (1), which is describing conservation of momentum, needs to be solved together with equation of mass continuity which for incompressible fluid reads

$$\nabla \cdot \mathbf{v} = 0 \quad (2)$$

Deformation of a structure is modeled by structural mechanics equation for displacement vector \mathbf{u}

$$\mathbf{f}_u = \rho \frac{\partial^2 \mathbf{u}}{\partial t^2} - \nabla \cdot \boldsymbol{\sigma} \quad (3)$$

where \mathbf{f}_u is a force acting on a differential volume and $\boldsymbol{\sigma}$ is a stress tensor. Stress $\boldsymbol{\sigma}$ and strain $\boldsymbol{\varepsilon}$ tensors are related through equation $\boldsymbol{\sigma} = \mathbf{c}_E \boldsymbol{\varepsilon}$, where \mathbf{c}_E is the elasticity matrix (determined with Young modulus of elasticity and Poisson ratio). Equations (1) to (3) are solved for fluid velocities and structural deformations together with supporting relations described in the text. After the pressure boundary condition was applied on the inlet, stationary direct fully-coupled solver was employed to solve structural deformation and stress in burst pressure test device. Outlet boundary condition velocity was set to zero, although model tolerates also non-zero outlet boundary condition, due to coupled fluidic module. Simulated magnitude of bond stress at applied inlet fluidic pressure of 50 kPa is shown in Fig. 5. Maximum stress was calculated at the region (presented with dark red color in Fig. 5) where fabricated test devices failed first (pointed out with arrow in Fig. 6), which positively validated simulation model.

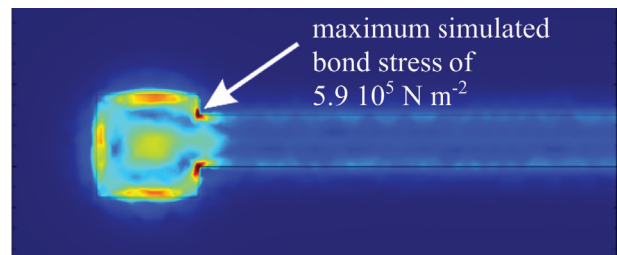


Figure 5: Simulated magnitude of bond stress at elevated fluidic pressure. Arrow indicates the point of maximum simulated bond stress.

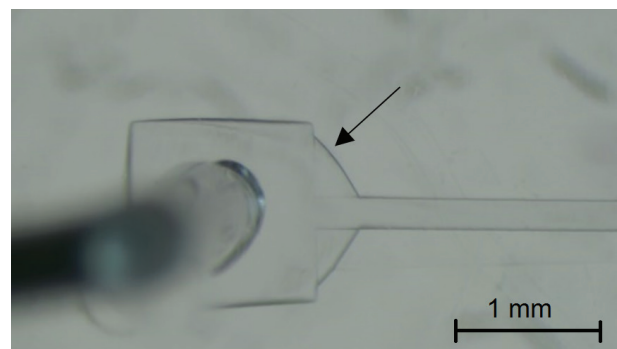


Figure 6: Micrograph of burst pressure test device. Arrow shows the failure onset region.

Simulation results show that the microfluidic channel design should avoid sharp edges throughout flow direction where layers delamination might be initiated.

3 Results

Since surfaces wettability is an essential criterion for inspecting the degree of surface activation in covalent bonding procedures, WCAs were measured first on raw and with O₂ plasma treated TP and PDMS surfaces. Results are presented in Table 1 (see also Fig. 1).

Table 1: WCAs for raw and oxygen plasma treated samples.

Polymer	raw	O2 plasma (1 min)	O2 plasma (5 min)
ABS	87	27	32
PC	74	38	37
PMMA	69	45	47
PDMS	87	4.5	/

Next, APTES (5%v/v in DI) was employed for functionalization of TP surfaces. With respect to others [2, 12] an additional post-deposition heat treatment and modified post-deposition plasma treatment were introduced in order to improve hydrolytic stability of covalent bonds. As expected, oxygen plasma treatment after modified APTES functionalization considerably improved surfaces wettability (see Table 2), which indicates high surface concentration of hydroxyl groups. However, wettability still declined considerably over time. In this study, no straightforward correlation between wettability of TP surfaces and TP-PDMS bond strength was found after the TP surfaces were functionalized.

Table 2: WCAs for APTES functionalized and oxygen plasma treated samples.

Polymer	APTES (5%v/v in DI)			Bond strength O2 plasma (20 sek)
	[°] 0 min	[°] after 30 min	[°] after 24 h	
ABS	9.5	38.7	74	accept.
PC	14.5	47	81	accept.
PMMA	12.3	36.5	83	accept.

In further investigation, 30 burst pressure tests employing water and compressed air were performed on fabricated PDMS test devices where TPs were previously functionalized with APTES or amine-PDMS linker. Again, no direct correlation between TP type (receiving equal surface preparation and bonding process) and bond strength was found. All test devices could sustain air pressures of 5 bars for at least 3 hours.

However, when burst pressure tests were performed by pressurized water, APTES devices started to fail immediately

after the fluidic pressure of 1 bar was applied with a channel edge delamination rate of 7.5 μm min⁻¹ in spite of additional post-deposition heat treatment and modification of post-deposition plasma treatment.

Similar hydrolysis of covalent bonds established via conventionally treated APTES was reported by Aran K et al. [12]. Results from testing bond strength under applied air pressure showed that the thermoplastics - PDMS bond was able to withstand more than 227.8 kPa, which was the maximum limit of their measuring equipment, without any sign of delamination. In further tests, the channels of the microdevices were filled with water and stored at room temperature for 72 h or the devices were filled and completely immersed in water for 72 h.

Surprisingly, the reported bonding strength for APTES coated membranes remained very strong (over 227.8 kPa) in devices stored at room temperature for 72 h with the device channels filled with water. However, complete immersion of the devices in water for an extended period of time weakened the membrane bonding strength for all of their tested bonding methods.

In another study, S. Kevin Lee et al. [2] reported bond failure and delamination of PDMS-APTES-TP sandwich structure after subjected to burst pressure test with water compressed above 15 psi.

An overview of silane is needed in order to understand the mechanisms for hydrolysis-induced bond failure. An organofunctional silane is a molecule comprising a silicon atom with at least one bond to carbon to enable organic functionality [6]. The inorganic side of the silane molecule consists of a silicon atom bound to alkoxy groups through Si—O—C linkages [2]. Hydrolytic instability of these bound alkoxy groups allows silanes to hydrolyze in the presence of water, converting the bound alkoxy groups to hydroxyl groups while liberating alcohol molecules. Any contact with water after bond formation will result in Si—O—C bond hydrolysis and ultimately bond failure [6, 13]. Furthermore, Si—O—C bonds have also been found to form directly between alkoxy groups such as methoxy and surface hydroxyl groups via alcoholysis [14]. Hydrolytic bond failure can occur at three locations in the bonding structure, at the thermoplastics-silane interface, at the PDMS-silane interface, and in the silane network itself [15]. While direct interface hydrolysis is unlikely due to the stability of the amide bond, any hydrophilic groups at the interface can act as nucleation sites for water condensation, allowing the silane network near the interface to be plasticized and weakened [16]. A similar process can occur at the PDMS-silane interface but with the possibility of hydrolysis directly at the inter-

face in addition to the weakening of the silane network [17]. For the silane network itself, high crosslink density can provide a major increase in resistance. However, networks formed by typical silanes, containing three silanol groups, tend to be cyclic, decreasing their resistance to dissolution [18]. Addressing failure mechanisms in all three locations is necessary to ensure hydrolytic stability [6,18].

In further investigation, burst pressure tests were performed on amine-PDMS linker test devices fabricated on PC, ABS and acrylic glass using pressurized water. Test devices withstood 2 bar water pressure for 3 hours without any delamination observed. Moreover, amine-PDMS linker devices were soaked in water for one week and successfully withstood all additional burst pressure tests. All tests confirmed hydrolytic stability of TP-PDMS bonds established through amine-PDMS linker. It is speculated that the water-repelling nature of the PDMS component in amine-PDMS linker prevented penetration of the aqueous solutions at the interface improving bond hydrolytic resistance [2, 3, 6].

Finally, developed bonding processes employing AP-TES and amine-PDMS linker were applied in modified micropump fabrication process. Based on the poor results of water tests on burst pressure devices, we further modified the APTES application by using multiple deposition steps (3 to 5 deposited layers), thus expecting the improvements of bonds hydrolytic resistance.

Our previously developed piezoelectric microcylinder pump prototypes [19] comprise activated PDMS elastomer layer bonded on its bottom side to the supporting bottom glass. Supporting bottom glass includes improvised fluidic connections and serves as a functional part of the micropump affecting micropump performance characteristics. Replacing supporting bottom glass with TP could pave the path toward micropump mass production in terms of enclosing the micropump in professional TP housing comprising professional fluidic and electric connections.

In the initial stage, supporting bottom glass was replaced with flat TP substrate. Exploded view of a typical TP microcylinder pump structure is shown in Fig. 7.

The TP microcylinder pump comprises PDMS elastomer layer with molded micropump chamber, fluidic microchannel and rectifying elements (Fig. 7 c). Additionally, two through-holes are punched into an elastomer, one into the center of the micropump chamber and the other one at the end of the channel. PDMS elastomer layer (Fig. 7 c) and PDMS fluidic connections (Fig. 7 e) are covalently bonded to the supporting TP substrate (Fig. 7 d) by employing developed multiple deposition

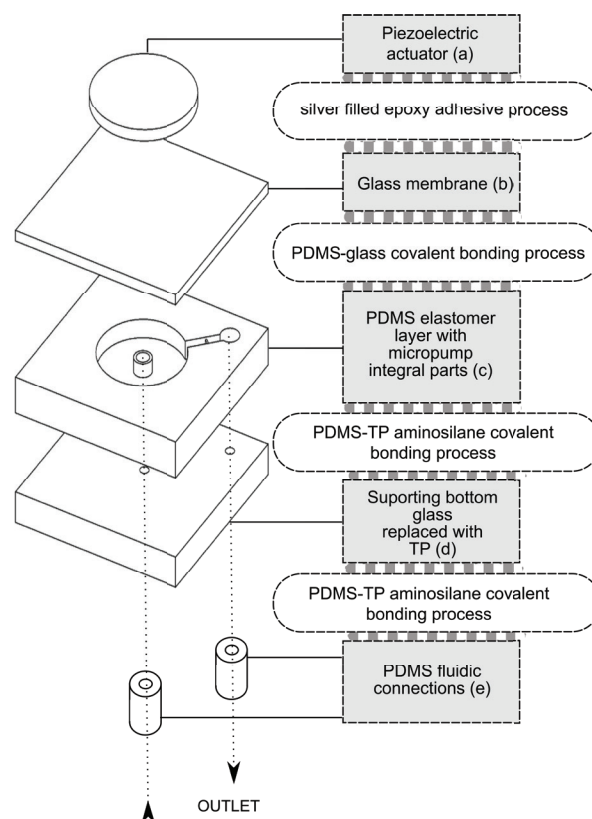


Figure 7: Exploded view of a typical TP microcylinder pump structure (dimensions are not to scale).

APTES or single deposition amine-PDMS linker bonding process.

One inlet and one outlet fluid port is drilled through a supporting TP substrate that supply and drain the fluid into and out of the pump. The micropump chamber and the microchannel are sealed with a thin glass membrane (Fig. 7 b) by employing oxygen plasma PDMS-glass covalent bonding process. Piezoelectric actuator (Fig 7 a) is positioned in the axis of a micropump chamber, coupled rigidly to the micropump membrane through silver filled epoxy adhesive (EPO-TEK EE129-4).

During excitation loosely attached glass membrane and PDMS elastomer layer deform in a controlled manner, which enables compression and expansion of the centrally placed inlet cylindrical port, micropump chamber and outlet throttle shaped port with a specific phase lag, contributing to efficient micropump operation.

Pumping test were performed by pumping air and DI water media. Both approaches passed air pumping tests, reaching maximum flow rate performance of 8 ml min⁻¹ and maximum backpressure performance of 100 mbar at applied square excitation waveform

with an amplitude of 140 V and a frequency of 300 Hz. However, during DI water pumping tests and despite improved multiple layer deposition process of APTES, micropumps degraded after several minutes of operation. This is depicted in Fig. 8 as APTES MP3 characteristics and further expanded on time scale in an in-set (see Fig. 8 central plot on the figure plane).

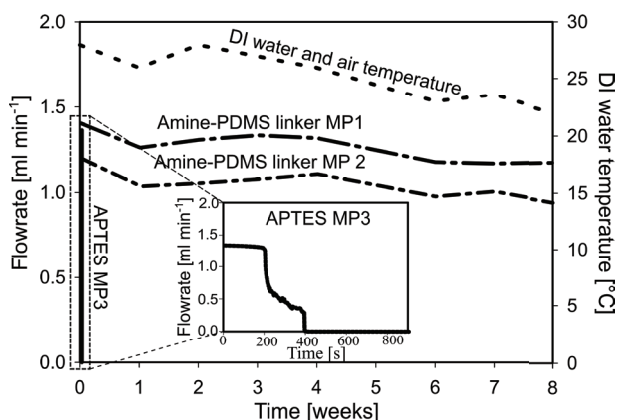


Figure 8: Long term flowrate stability characteristics of three representative micropump devices and ambient temperature.

In contrast, amine-PDMS linker composed of a PDMS backbone incorporating an amine side group established hydrolytically stable covalent bonds. This was confirmed by long-term flowrate stability measurements on two micropumps MP1 and MP2 with typical performances yielding initial maximum DI water flowrate performance of 1.2 ml min^{-1} and 1.4 ml min^{-1} at applied RC excitation waveform [20] with an amplitude of 140 V and a frequency of 300 Hz. Figure 8 also includes measurement setup ambient temperature (dotted line closest to the upper edge of the diagram). Due to partial correlation between flowrate performance characteristics of MP1 and MP2 and measurement setup ambient temperature it was concluded that transient deviations in flowrate characteristics are to be attributed to temperature changes of the medium viscosity, the micropump and driving electronics throughout the measurement. Therefore, long term stability measurements should be improved by setting measuring setup in a temperature stabilized chamber. Micropumps employing amine-PDMS linker bonding process exhibit no deterioration in their performance after eight weeks of continuous operation.

4 Conclusions

Low temperature process for TP-PDMS irreversible covalent bonding was presented. Process is based on silylation of the TP surfaces through the use of orga-

nonfunctional silanes. As the silanol groups are polar in nature, they make the exposed surface highly hydrophilic and this was observed by measuring WCAs. However in this study, no direct correlation between wettability of TP surfaces deposited with APTES and final bond strength was found. In further investigation, burst pressure tests were performed on designed and fabricated PDMS test devices employing TPs functionalized with APTES or amine-PDMS linker. All devices sustained air pressures of 5 bars for at least 3 hours, but only amine-PDMS linker test devices sustained continuous water pressure as high as 2 bars without delamination. Bonds established via APTES and subjected to water decayed in spite of additional post-deposition heat treatment and modification of post-deposition plasma treatment. In further application oriented study, both bonding processes were applied on piezoelectric micropumps where glass substrate was replaced by thermoplastic substrate. Even implementation of multiple deposition steps of APTES was insufficient in preventing hydrolysis of covalent bonds, resulting in micropumps performance deterioration. On the other hand, micropumps employing amine-PDMS linker exhibit no deterioration in their performance even after eight weeks of continuous operation.

5 Acknowledgments

Authors would like to thank the Slovenian Research Agency/ARRS (P2-0105, P2-0244), Ministry of Education, Science and Sport and Kolektor Group d.d. for their support of this work.

6 References

1. Yetisen, A. K., Akram, M. S., & Lowe, C. R. (2013). Based microfluidic point-of-care diagnostic devices. *Lab on a Chip*, 13(12), 2210-2251.
2. Lee, S. K., Lee, H., & Ram, J. R. (2016). U.S. Patent No. 9,422,409. Washington, DC: U.S. Patent and Trademark Office.
3. Wu, J., & Lee, N. Y. (2014). One-step surface modification for irreversible bonding of various plastics with a poly (dimethylsiloxane) elastomer at room temperature. *Lab on a Chip*, 14(9), 1564-1571.
4. Suzuki, Y., Yamada, M., & Seki, M. (2010). Sol-gel based fabrication of hybrid microfluidic devices composed of PDMS and thermoplastic substrates. *Sensors and Actuators B: Chemical*, 148(1), 323-329.
5. Tsao, C. W., & DeVoe, D. L. (2009). Bonding of thermoplastic polymer microfluidics. *Microfluidics and Nanofluidics*, 6(1), 1-16.

6. Lee, K. S., & Ram, R. J. (2009). Plastic–PDMS bonding for high pressure hydrolytically stable active microfluidics. *Lab on a Chip*, 9(11), 1618-1624.
7. Tang, L., & Lee, N. Y. (2010). A facile route for irreversible bonding of plastic-PDMS hybrid microdevices at room temperature. *Lab on a Chip*, 10(10), 1274-1280.
8. Karakoy, M., Gultepe, E., Pandey, S., Khashab, M. A., & Gracias, D. H. (2014). Silane surface modification for improved bioadhesion of esophageal stents. *Applied surface science*, 311, 684-689.
9. Garbassi, F., Morra, M., Occhiello, E., & Garbassi, F. (1998). *Polymer surfaces: from physics to technology* (pp. 169-200). Chichester: Wiley.
10. Hillborg, H., & Gedde, U. W. (1999). Hydrophobicity changes in silicone rubbers. *IEEE Transactions on Dielectrics and Electrical insulation*, 6(5), 703-717.
11. Bhattacharya, S., Datta, A., Berg, J. M., & Gangopadhyay, S. (2005). Studies on surface wettability of poly (dimethyl) siloxane (PDMS) and glass under oxygen-plasma treatment and correlation with bond strength. *Journal of microelectromechanical systems*, 14(3), 590-597.
12. Aran, K., Sasso, L. A., Kamdar, N., & Zahn, J. D. (2010). Irreversible, direct bonding of nanoporous polymer membranes to PDMS or glass microdevices. *Lab on a Chip*, 10(5), 548-552.
13. Goebel, R. (2003). U.S. Patent No. 6,613,439. Washington, DC: U.S. Patent and Trademark Office.
14. Pape, P. G., & Plueddemann, E. P. (1991). Methods for improving the performance of silane coupling agents. *Journal of adhesion science and technology*, 5(10), 831-842.
15. Plueddemann, E. P. (1991). Reminiscing on silane coupling agents. *Journal of Adhesion Science and Technology*, 5(4), 261-277.
16. Tesoro, G., & Wu, Y. (1991). Silane coupling agents: the role of the organofunctional group. *Journal of adhesion science and technology*, 5(10), 771-784.
17. Battjes, K. P., Barolo, A. M., & Dreyfuss, P. (1991). New evidence related to reactions of aminated silane coupling agents with carbon dioxide. *Journal of Adhesion Science and Technology*, 5(10), 785-799.
18. Plueddemann, E. P. (1991). Adhesion through silane coupling agents. In *Fundamentals of adhesion* (pp. 279-290). Springer US.
19. Dolžan, T., Pečar, B., Možek, M., Resnik, D., & Vrtačnik, D. (2015). Self-priming bubble tolerant microcylinder pump. *Sensors and Actuators A: Physical*, 233, 548-556.
20. http://www.electronics-tutorials.ws/rc/rc_3.html (17.10.2017)

Arrived: 31. 08. 2017

Accepted: 26. 10. 2017